Synthesis and interfacial activity of PMMA/PtBMA Janus and homogeneous nanoparticles at water/oil interfaces.

Miguel Angel Fernandez-Rodriguez,[1,*] Sahar Rahmani,[2,3,6] Chris K. J. Yu,[2,5] Miguel Angel Rodriguez-Valverde,[1] Miguel Angel Cabrerizo-Vilchez,[1] Charnelle A. Michel,[2,4]Joerg Lahann[2-6] and Roque Hidalgo-Alvarez[1]

*e-mail: mafernandez@ugr.es

[1]Biocolloid and Fluid Physics Group, Applied Physics Department, Faculty of Sciences, University of Granada, 18071 Granada, Spain.
[2]Biointerfaces Institute, University of Michigan, Ann Arbor, MI 48109, USA
[3]Biomedical Engineering, University of Michigan, Ann Arbor, MI 48109, USA
[4]Chemical Engineering, University of Michigan, Ann Arbor, MI 48109, USA
[5]Material Science & Engineering, University of Michigan, Ann Arbor, MI 48109, USA
[6]Institute of Functional Interfaces (IFG), Karlsruhe Institute of Technology (KIT), Karlsruhe, Germany

KEYWORDS: Electrohydrodynamic co-jetting; PMMA/PtBMA; Janus nanoparticles; Interfacial activity; Pendant drop tensiometry.

ABSTRACT

Polymethylmethacrylate/Poly-*tert*-butylmethacrylate Janus nanoparticles were synthesized by the electrohydrodynamic co-jetting method. The Janus character of these nanoparticles was visualized through super-resolution imaging with Structured Illumination Microscopy. The Janus nanoparticles, and the corresponding homogeneous sets, were then morphologically characterized to assess their size, distribution, and concentrations. All nanoparticles presented high interfacial activity as measured by pendant drop tensiometry at water/decane interfaces. At high concentrations and compression states, the Janus nanoparticles exhibited higher interfacial activity than the homogeneous nanoparticles. This is in agreement with theoretical and

experimental works in which Janus nanoparticles present higher interfacial activity than homogeneous nanoparticles.

Introduction:

Janus nanoparticles are of interest when designing fluid interfaces covered by nanoparticles due to their improved interfacial activity over homogeneous nanoparticles (1). Polymeric Janus nanoparticles can induce spontaneous self-assembly at interfaces due to the contrast between their spatial domains and can even be responsive to external magnetic/electric fields, pH/temperature gradients, and light (2; 3; 4; 5; 6; 7). Such nanoparticles have a theoretical higher stability at liquid-liquid interfaces as compared to their homogenous counterparts and can act as surfactants to stabilize such systems (1). There are three main strategies to synthesize Janus nanoparticles with polymeric capping ligands concerning the core and capping ligand constituents. The first involves the selective functionalization of an inorganic or polymeric core with different polymers in each hemisphere as capping ligands (8; 9; 10). The second approach consists of selective polymerization over an inorganic core (11; 12; 13) and the laststrategy involves the selective polymerization of entirely Janus polymeric nanoparticles (3; 4; 5; 6; 7; 14). Outside of these methods that focus on controlling the capping ligands, another possible technique to fabricate Janus nanoparticles is the template-assisted synthesis in which a bulk film of block terpolymers is cross-linked (15). Depending on the affinity of the polymer constituents to water or oil, it is possible to produce amphiphilic polymeric Janus particles with enhanced interfacial activity (14). A more versatile technique for the synthesis of Janus nanoparticle is Electrohydrodynamic (EHD) Co-Jetting, which has been shown to be able to incorporate a variety of different polymers in each phase (8; 16). This technique can be used to fabricate

nanoparticles and fibers with multiple compartments, each of which can contain a different polymer or perhaps encapsulate a different molecule (16; 17; 18). With respect to self-assembly applications, this technique is advantageous due to its ability to incorporate a wide range of polymers into each hemisphere of the particles regardless of the polymers' amphiphilic nature or polymerization techniques, which can be a limiting factor in other particle fabrication techniques (19; 20; 21; 18).

Previous studies showed that Janus nanoparticles can be used for self-assembly applications (15; 22; 23; 24). Ruhland et al. (15) synthesized polymeric Janus nanoparticles with different morphologies with the template-assisted technique. They studied the enhanced self-assembly of their Janus nanoparticles at water/toluene interfaces by pendant drop tensiometry. Similarly, Park et al. (22) synthesized and studied homogeneous polystyrene (PS) nanoparticles and gold-coated PS Janus nanoparticles at water/decane interfaces. Whereas the homogeneous PS nanoparticles exhibited a hexagonal lattice at the water/decane interface, the Janus nanoparticles aggregated in fractal structures. Furthermore, Nie et al. (23) found that amphiphilic polymeric JPs assembled into supermicelles. The Janus clusters seem to keep the asymmetry charge and Janus character, acting as larger Janus nanoparticles (24).

In this work, we employed polymethylmethacrylate and poly-tert-butylmethacrylate as the polymers incorporated into our nanoparticles because they exhibit a large contact angle difference (of water in a polymer coated silicon wafer): 68º (25) and 108º (26), respectively. Thus, they are expected to have interfacial activity. We synthesized homogeneous spherical nanoparticles made of the mentioned polymers and Janus nanoparticles with the polymers separated in two hemispheres by Electrohydrodynamic co-jetting. The nanoparticles were

characterized by SEM, DLS, and super-resolution imaging with Structured Illumination Microscopy (SIM) to determine their size, shape, concentration, and compartmentalized nature. The interfacial activity at water/decane interfaces and interfacial dilatational rheology was studied by pendant drop tensiometry.

Experimental section:

Materials: Polymethylmethacrylate (PMMA) with a molecular weight of 20 kDa, hexadecyltrimethylammonium bromide (CTAB), chloroform, dimethylformamide (DMF), poly(9,9-dioctylfluorene-*alt*-benzothiadiazole) (green dye), and decane HPLC were purchased from Sigma Aldrich, USA. Poly-tert-butylmethacrylate(PtBMA) was purchased from Polysciences, USA, and ADS306PT (red dye) was purchased from American Dye Source, Canada. ProLong Gold antifade reagent was provided by Life Technologies.

Janus and homogeneous nanoparticles fabrication and characterization: Nanoparticles were fabricated through the Electrohydrodynamic Co-Jetting process by flowing multiple polymeric solutions through metal capillaries in a side-by-side configuration (8; 16). The flows were kept under a laminar regime and at the tip of the capillaries the solutions came together to form a droplet, to which an electric voltage was applied. The application of the electric field caused the solutions to form a Taylor cone, which created a spray of individual droplets that accelerated towards the counter electrode. During this process, the surface area to volume ratio of the nanoparticles decreased rapidly and the solvents used evaporated quickly resulting in polymeric nanoparticles deposited on the counter electrode. Due to the rapid evaporation of the solvents and the laminar regime used, the solvents did not have sufficient time to mix and the resulting nanoparticles displayed individual compartments made of each polymer solution instead of a

mixture of all solutions used. In this manuscript, Janus nanoparticles were fabricated by using two laminar flows, each of which contained a different polymer (one flow contained PMMA while the other contained PtBMA). For the PMMA compartment a polymer concentration of 5% w/v, a hexadecyltrimethylammonium bromide (CTAB) concentration of 2.5% w/v, and a solvent ratio of 70:30 chloroform:DMF was used. For the PtBMA compartment, a polymer concentration of 5% w/v, a CTAB concentration of 2.5% w/v, and a solvent ratio of 85:15 was used. For homogeneous nanoparticles composed of each neat polymer the same solvent ratios were used, respectively. The flow rate used for all nanoparticles was 0.1 ml per hour with a distance of 35 cm between the needles and the counter electrode. Once fabricated, the nanoparticles were analyzed with Scanning Electron Microscopy (SEM) to determine their size and shape, and ImageJ analysis to determine their size distribution.

Structured Illumination Microscopy (SIM) of Janus Nanoparticles: Janus nanoparticles with a separate dye in each compartment (red and green) were fabricated as described above. The nanoparticles were directly jetted onto glass cover slips and were incubated in ProLong Gold antifade reagents overnight before imaging with a Zeiss Structured Illumination Microscope to demonstrate their bicompartmental nature.

Nanoparticle Isolation and Characterization: The nanoparticles were collected in DI water and separated via centrifugation at 3220 RCF for 6 hours to isolate the desired fraction. Their size distribution was analyzed via Dynamic Light Scattering (DLS) and their concentration was determined based on Nanoparticle Tracking Analysis (NTA) using Nanosight equipment. The electrophoretic mobility was measured using a Malvern Zetasizer. Before use for particle analysis measurements, the nanoparticles were washed multiple times with DI water in glass

containers to remove any trace of CTAB present in the solutions to eliminate any interference this molecule might have with the experiments.

Pendant drop tensiometry: This is an extensively employed method for characterizing surface and interfacial tension of liquids (27). The pendant drop experiments were performed in a similar way as previous work with gold Janus nanoparticles (28): first we deposited a given amount of nanoparticle dispersion with a microsyringe on an initial 20 μl MilliQ water pendant drop in air. Next, the pendant drop was shrunk down to 10 μl to immerse the capillary in decane (see Fig. 4a and 4b). The immersion in decane provided a lower bare interfacial tension and thus a better adsorption of the particles at the interface (29). Next, the pendant drop was grown to 45 μl inside the decane phase (see Fig. 4c) and the interfacial tension was monitored during a one-hour period to reach the stabilization of the interfacial tension. This interfacial tension stabilization was performed for three initial concentration of nanoparticles deposited at the pendant drop interface in separate experiments. Each sample was normalized to have the same total surface area at the pendant drop interface (assuming that all nanoparticles assembled at the interface in a close-packed configuration) by taking into account the individual surface area of each nanoparticle and the concentration of each sample as measured by NTA analysis. The two total surfaces areas explored were $(3.08\pm0.08)\cdot10^{-6}$ m^2 and $(6.15\pm0.16)\cdot10^{-6}$ m^2. Finally, we performed growing and shrinking experiments in which the interfacial pressure $\Pi=\gamma_0-\gamma$ (where γ_0 is the interfacial tension of pure water/decane, 52.3 mN/m, and γ is the interfacial tension) was plotted against the pendant drop area.

Additionally, interfacial dilatational rheology was performed by performing growing and shrinking of the pendant drop at different periods and amplitude of 1 μl. The phase and amplitude difference between the input sinusoidal wave and the output interfacial tension wave

can be expressed as a complex dilatational modulus which accounts for the change in the surface tension γ when there is a change in the interface area A.

$$\frac{d\gamma}{d(\ln A)} = E + i\frac{2\pi}{T}\eta \qquad (1)$$

Equation 1 enables to estimate the interfacial dilatational elastic modulus E and viscosity η, for a given period of oscillation T, as in previous works (30). These measurements were made at the water/air interface because the behavior was the same in both water/air and water/decane interfaces but the signal-to-noise ratio was higher at water/air interfaces.

Results and discussion:

The homogeneous nanoparticles made of polymethylmethacrylate (labeled as PMMA), poly-tert-butylmethacrylate (labeled as PtBMA), and the Janus nanoparticles with PMMA in one hemisphere and PtBMA in the second hemisphere (labeled as Janus particles or JPs) were synthesized by Electrohydrodynamic (EHD) co-jetting (8; 16). This technique was represented in Fig. 1a. Briefly, polymeric solutions were flown in a laminar regime through metal capillaries. An electric current was applied to the tip of the capillaries and the charged solutions formed into a Taylor cone. At the tip of this cone, a spray of droplets accelerated toward the counter electrode. Due to the rapid evaporation of the solvents, the reduction in the surface to volume ratio, and the speed of the jet, the solutions did not have sufficient time to mix and the resulting particles retain their flow-determined configurations. As a result, particles with individual compartments were deposited on the counter electrode. To create the nanoparticles instead of microparticles, the solution parameters were changed to increase the dielectric constant of the jetted material. Specifically, a higher ratio of dimethylformamide (dielectric constant of 38) than

chloroform (dielectric constant of 4.81) and a charged surfactant (CTAB) were employed to change the solution characteristics. Based on these changes, the nanoparticles obtained had significantly monodispersed populations as it can be observed by SEM imaging (Fig. 1b-d). The as fabricated nanoparticles had the following average diameters and distributions based on ImageJ analysis of Scanning Electron Microscopy (SEM) images of over 500 nanoparticles: (i) PMMA homogenous nanoparticles: 101 ± 51 nm; (ii) PtBMA homogenous nanoparticles: 82 ± 33 nm; (iii) Janus nanoparticles: 90 ± 40 nm.

To demonstrate the compartmental nature of the Janus particles, super-resolution imaging with Structured Illumination Microscopy (SIM) was done. These particles contained a green dye in the PtBMA compartment and a red dye in the PMMA compartment. As demonstrated in Fig. 2, the dyes were in two distinct regions of these particles, signifying the two separated compartments.

To create a more monodispersed solution of particles and remove any potential aggregates, fractionation via centrifugation was used. In this technique, the larger particles were removed at lower centrifugation times/durations, while the smaller sized particles were isolated at longer durations and higher speeds. To isolate the nanoparticles for this study, nanoparticles were centrifuged at 3220 RCF for 6 hours, followed by several washes with DI water at the same settings. The average hydrodynamic size after fractionation was similar for each nanoparticle and in the range of 200 nm in diameter, as measured by DLS (see Fig.3) and Nanoparticle Tracking Analysis (NTA) (table in Fig. 3). Specifically, based on NTA measurements the nanoparticles averaged at a diameter of 163±39nm for PMMA nanoparticles, 217±40 nm for PtBMA nanoparticles, and 172±28 nm for the Janus nanoparticles. The total concentration of the

nanoparticle, which was then used to determine the surface area of each sample, was measured via NTA analysis.

The main differences between classical surfactants and Janus nanoparticles come from their size, rigid character and wettability contrast. Thus, the adhesion energy increases with the squared radius of the object attached at the interface (1), the rigid character also difficult the spatial reconfiguration of the nanoparticles at the interface compared to the classical surfactants when the interface become shrunk or subjected to dilatational rheology and it is possible to design a specific wettability contrast to maximize their interfacial activity in a given interface. Those factors support the idea of the Janus particles presenting higher interfacial activity compared to classical surfactants. The interfacial activity of the nanoparticles was characterized by pendant drop tensiometry (see Fig. 4) (28). The interfacial tension for different total surface areas of nanoparticles was represented in Fig. 5a and 5b. As explained in the Experimental Section, for all experiments, the pendant drop was maintained to a constant drop volume of 45 μl during 1 hour previous to the growing and shrinking experiments. Since the spreading solvent was water, as well as the pendant drop, we could expect a Gibbs monolayer in which the nanoparticles were placed in the bulk and had to reach the interface in a slow process compared to laboratory timescales (31). However, in the laboratory timescale the growing and shrinking experiments showed closed hysteresis cycles (see Fig. 5a and 5b). Thus, the interfacial tension evolved in such a slow pace that for the entire experiment this change was negligible. The PMMA nanoparticles showed the lowest interfacial pressures and the PtBMA and Janus nanoparticles exhibited the similar interfacial pressure at the right end where it coincided with the more expanded area of the pendant drop. Nevertheless, upon compression, the Janus nanoparticles reached higher interfacial pressure than the PtBMA nanoparticles. This was in agreement with

the theoretical prediction that a Janus nanoparticle with equal hydrophilic and hydrophobic areas present three times more surface activity than the corresponding homogeneous particles at a water/oil interface and previous experimental results in which Janus nanoparticles presented higher interfacial activity than homogeneous nanoparticles (1; 28; 30). In our case, despite the Super-resolution images in Fig. 2, we cannot confirm that our particles have equal hydrophilic and hydrophobic areas and it is expected slightly lower interfacial activity compared to Janus particles with equal hydrophilic and hydrophobic areas (1). Nevertheless, putting double number of particles to obtain an estimated double area coverage at the pendant drop surface did not result in an enhanced interfacial activity probably due to the fact that these nanoparticles already self-assembled at the interface with the lower number of nanoparticles deposited, offering an enhanced interfacial activity. Thus, the PMMA/PtBMA Janus nanoparticles seemed to be better emulsifiers than the homogeneous PtBMA or PMMA nanoparticles because of their enhanced interfacial activity. Given the quantity of studies devoted to PMMA and PtBMA laden interfaces, we were interested in developing a deeper characterization of the PMMA/PtBMA Janus behavior at interfaces. As explained in the Experimental Section, the interfacial dilatational rheology was performed for different area per particle (i.e. different monolayer compression states) at water/air interfaces after testing that the behavior was the same at both water/decane and water/air interfaces but with lower signal-to-noise ratio at water/decane interfaces. The results of interfacial dilatational elastic modulus E and viscosity η were plotted in Fig. 6 against different periods for different areas per particle. It could be seen that E decreased and η increased with increasing periods. This could be explained in terms of the perturbations, where higher periods produced slower perturbations that resulted in less elastic and more viscous interfaces. Moreover, upon compression (i.e. lower area per particle) E and η increased clearly, pointing out an elastic

shell behavior of the particle-laden interface. This elastic shell behavior pointed out the ability of these particles as emulsifiers as they were strongly adsorbed at the interfaces.

Conclusions:

Polymethylmethacrylate/Poly-tert-butylmethacrylate (PMMA/PtBMA) Janus nanoparticles were fabricated via the Electrohydrodynamic co-jetting process. The Janus character of the nanoparticles was demonstrated by super-resolution imaging with Structured Illumination Microscopy, in which the two compartments were observed in separate regions. The Janus nanoparticles, and the corresponding homogeneous nanoparticles of PMMA and PtBMA, were characterized by SEM, Nanoparticle Tracking Analysis, and DLS, which revealed relatively monodispersed nanoparticle dispersions with diameters in the range of 160-200 nm. The interfacial activity of these nanoparticles was studied via pendant drop tensiometry by the deposition of nanoparticles in water pendant drops and subsequent immersion in decane. The Janus nanoparticles and PtBMA homogeneous nanoparticles exhibited similar interfacial activity for the more expanded state of the pendant drop and were always higher than the PMMA homogeneous nanoparticles. Nevertheless, upon compression the Janus nanoparticles reached higher interfacial pressures for growing and shrinking pendant drop experiments, demonstrating their capability as emulsifiers. Moreover, the interfacial dilatational rheology of such nanoparticles showed an elastic shell behavior that also demonstrates the ability of these particles as emulsifiers. With these characteristics, such Janus nanoparticles could potentially be used to replace traditional emulsifiers in the future.

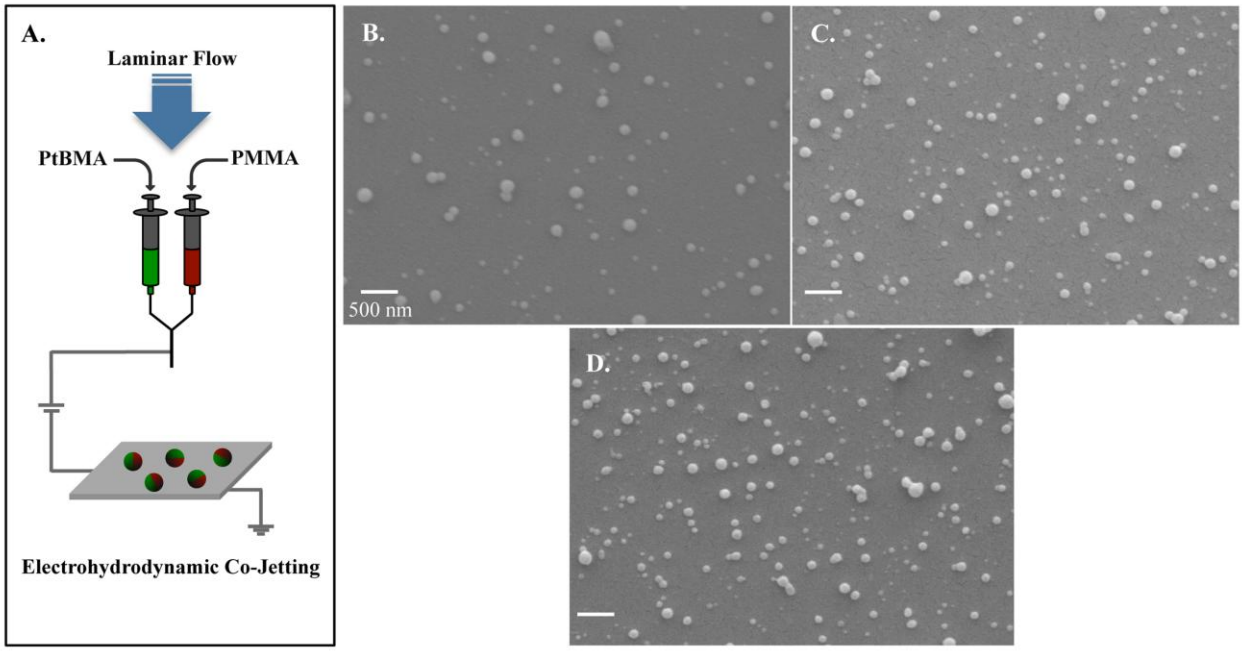

Figure 1: Fabrication of nanoparticles and their size characterization. (A) Schematic of Electrohydrodynamic co-jetting of Janus nanoparticles. (B-D) SEM images of the as-fabricated PMMA, PtBMA, and Janus nanoparticles, respectively. All scale bars are 500 nm.

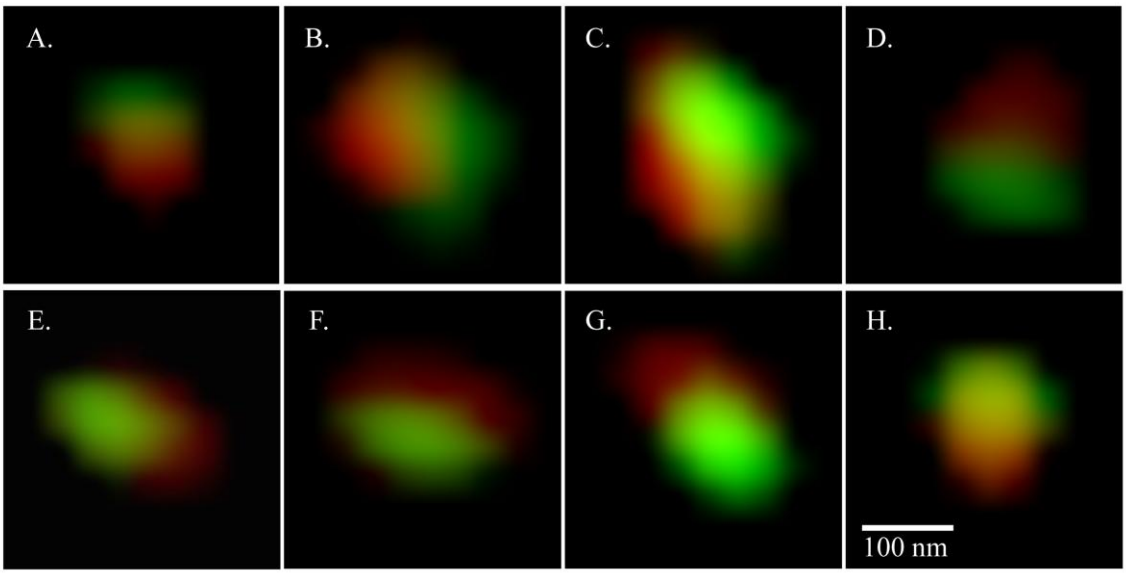

Figure 2: Super-resolution imaging of Janus nanoparticles with Structured Illumination Microscopy. (A-H) Images of specific Janus nanoparticles demonstrating their bicompartmental nature, where the green and red dyes are in separate regions of each nanoparticle. All images are from the same original file and have been resized to the same pixel width.

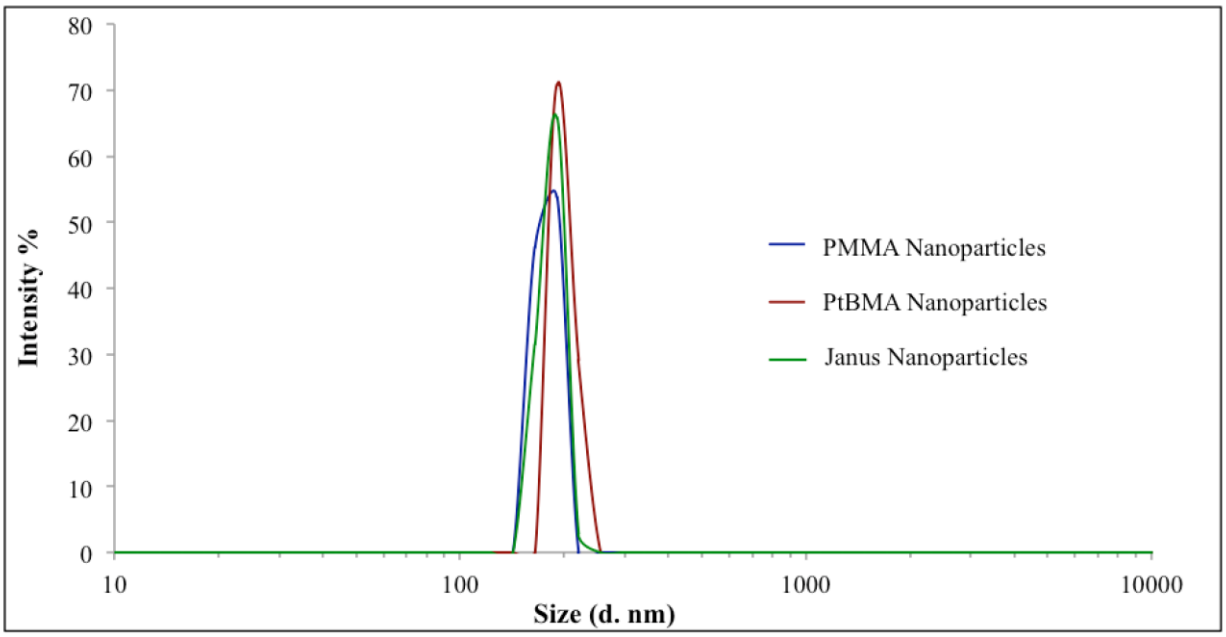

Nanoparticle	Average size (d. nm)
PMMA	163± 39
PtBMA	217± 40
Janus Nanoparticles	172± 28

Figure 3: Particle analysis after fractionation into a specific size range via centrifugation. Top: Size distribution of each set of nanoparticles based on DLS (Dynamic Light Scattering) analysis. Bottom: Table with average diameter based on NTA (Nanoparticle Tracking Analysis) measurements for each particle set.

(A) (B) (C)

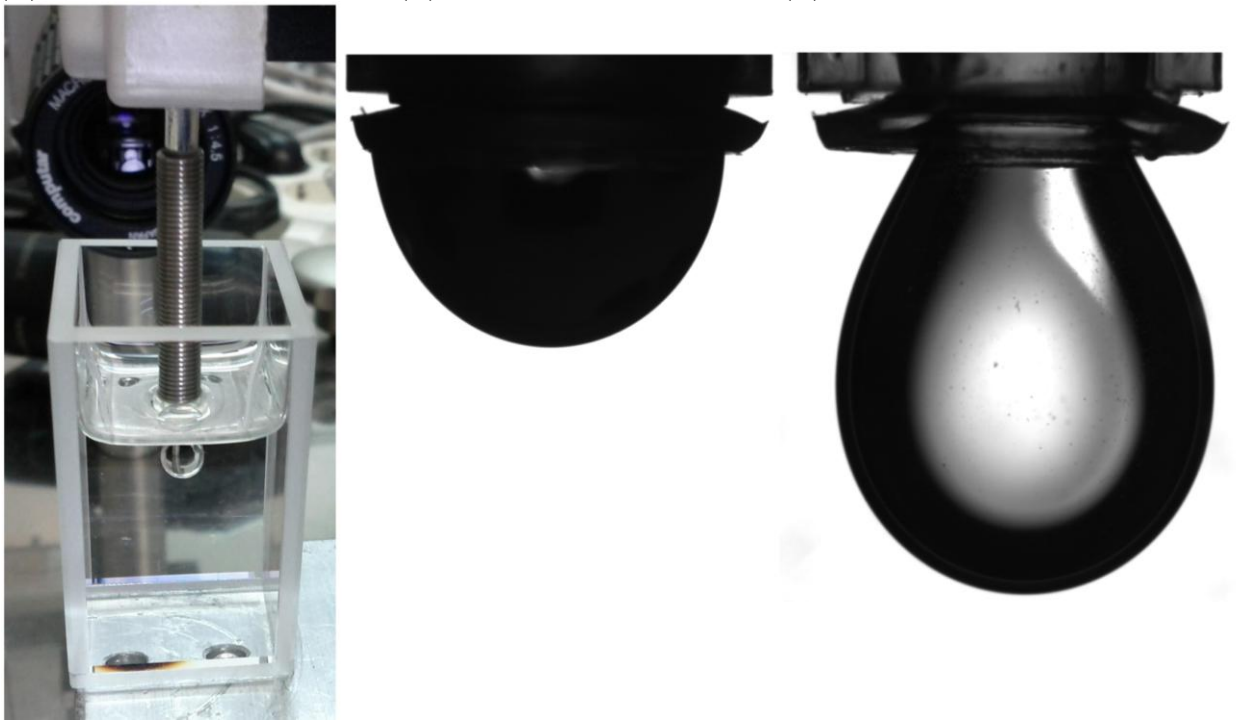

Figure 4. (A) Experimental setup. (B) A 10 µl water pendant drop with Janus nanoparticles just before immersion in decane. (C) Same pendant drop as (B) is grown to 45 µl immersed in decane.

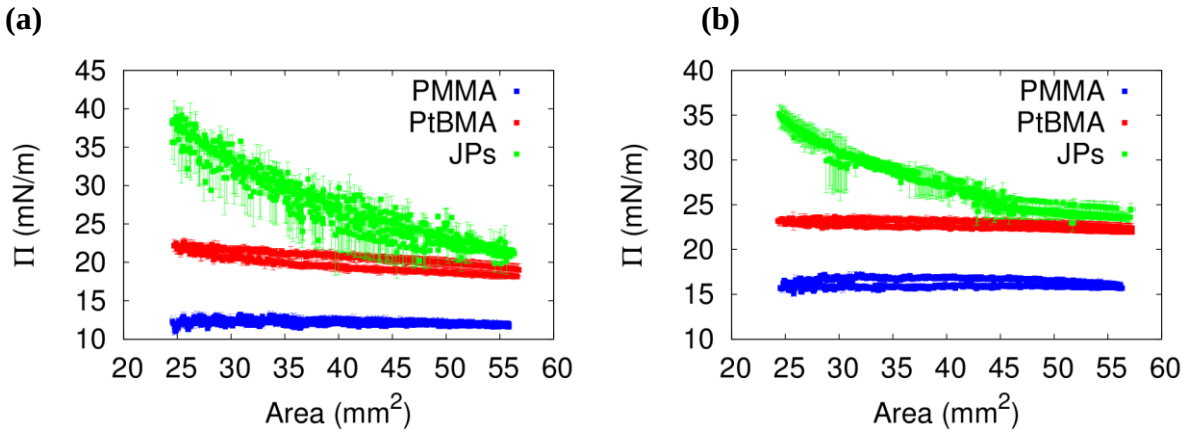

Figure 5. Growing and shrinking cycles corresponding to water pendant drops immersed in decane with different surface area coverage [$(3.08\pm0.08)\cdot10^{-6}$ m^2 for **5a** and $(6.15\pm0.16)\cdot10^{-6}$ m^2 for **5b**] of PMMA, PtBMA and Janus Nanoparticles (JPs). The interfacial pressure is plotted against the pendant drop area.

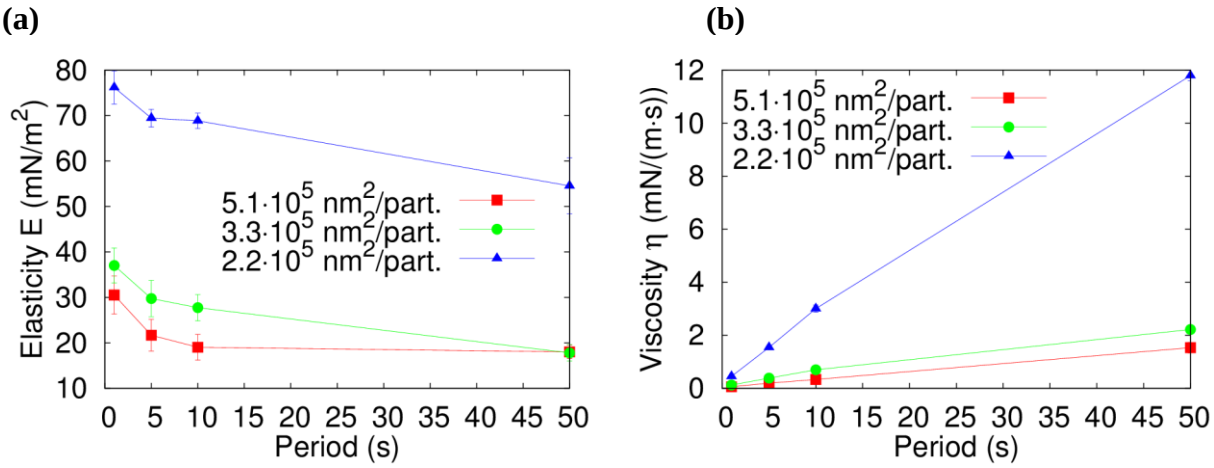

Figure 6. Interfacial dilatational **(a)** elastic modulus E and **(b)** viscosity η against different periods and 1 µl amplitude for different areas per PMMA/PtBMA Janus nanoparticle at the water/air interface.

ACKNOWLEDGMENT

This work was supported by the Spanish MINECO [projects MAT2011-23339 and MAT2013-44429-R], by "Junta de Andalucía" and FEDER [projects P10-FQM-5977 and P12-FQM-1443], Multidisciplinary University Research Initiative of the Department of Defense, and the Army Research Office [W911NF-10-1-0518], the DOD through an idea award [W81XWH-11-1-0111], the Tissue Engineering and Regenerative Medicine Training Grant [DE00007057-36], and the European Community's Seventh Framework Programme [FP7/2007-2013] under grant agreement nº 310445 [SAVVY]. The authors thank J.A. Holgado-Terriza and J.L. Muros-Cobos for the software Dinaten© used for the interfacial tension measurements.

REFERENCES

1. Binks BP, Fletcher PDI. Particles Adsorbed at the Oil-Water Interface: A Theoretical Comparison between Spheres of Uniform Wettability and Janus Particles. Langmuir 2001; 17:4708-10.
2. Bradley M, Rowe J. Cluster formation of Janus polymer microgels. Soft Matter 2009; 5:3114-9.
3. Kaewsaneha C, Tangboriboonrat P, Polpanich D, Eissa M, Elaissari A. Facile method for preparation of anisotropic submicron magnetic Janus particles using miniemulsion. J. Colloid Interface Sci. 2013; 409:66-71.
4. Faita FL, Trindade AC, Godinho MH, Bechtold IH. Luminescent elastomeric Janus particles. J. Colloid Interface Sci. 2013; 410:124-130.
5. Kaewsaneha C, Bitar A, Tangboriboonrat P, Polpanich D, Elaissari A. Fluorescent-magnetic Janus particles prepared via seed emulsion polymerization. J. Colloid Interface Sci. 2014; 424:98-103.
6. Nisisako T. Recent advances in microfluidic production of Janus droplets and particles. Curr. Opin. Colloid Interface Sci. 2016; 25:1-12.
7. Zhai W, Wang B, Wang Y, He Y-F, Song P, Wang R-M. An efficient strategy for preparation of polymeric Janus particles with controllable morphologies and emulsifiabilities. Colloids Surf. A 2016; 503:94-100.
8. Walther A, Müller AHE. Janus Particles: Synthesis, Self-Assembly, Physical Properties, and Applications. Chem. Rev. 2013; 113:5194-261.
9. Sashuk V, Hołyst R, Wojciechowski T, Fiałkowski M. Close-packed monolayers of charged Janus-type nanoparticles at the air-water interface. J. Colloid Interface Sci. 2012; 375(1):180-6.

10. Luo K, Xiang Y, Wang H, Xiang L, Luo Z. Multiple-Sized Amphiphilic Janus Gold Nanoparticles by Ligand Exchange at Toluene/Water Interface. J. Mater. Sci. Technol. 2016,32(8):733-737.
11. Qiang W, Wang Y, He P, Xu H, Gu H, Shi D. Synthesis of Asymmetric Inorganic/Polymer Nanocomposite Particles via Localized Substrate Surface Modification and Miniemulsion Polymerization. Langmuir 2008; 24:606-608.
12. Liu L, Ren M, Yang W. Preparation of Polymeric Janus Particles by Directional UV-Induced Reactions. Langmuir 2009; 25:11048-53.
13. Ge X, Wang M, Yuan Q, Wang H, Ge X. The morphological control of anisotropic polystyrene/silica hybrid particles prepared by radiation miniemulsion polymerization. Chem. Commun. 2009;2765-2767.
14. Li C, Wu Z, He YF, Song PF, Zhai W, Wang RM. A facile fabrication of amphiphilic Janus and hollow latex particles by controlling multistage emulsion polymerization. J. Colloid Interface Sci. 2014; 426:39-43.
15. Ruhland TM, Grüschel AH, Ballard N, Skelhon TS, Walther A, Müller AHE, Bon SAF. Influence of Janus Particle Shape on Their Interfacial Behavior at Liquid-Liquid Interfaces. Langmuir 2013; 29:1388-94.
16. Roh KH, Martin DC, Lahann J. Biphasic Janus particles with nanoscale anisotropy. Nat Mater. 2005;4(10):759-63.
17. Rahmani S, Ross AM, Park TH, Durmaz H, Dishman AF, Prieskorn DM, Lahann J. Dual Release Carriers for Cochlear Delivery. Adv. Healthcare Mat. 2016; 5(1):94-100.
18. Lee KJ, Yoon J, Rahmani S, Hwang S, Bhaskar S, Mitragotri S, Lahann J. Spontaneous Shape Reconfiguration in Multicompartmental Microcylinders. Proc. Natl. Acad. Sci. U.S.A. 2012; 109(40):16057-62.
19. Sokolovskaya E, Rahmani S, Misra AC, Bräse S, Lahann J. Dual-Stimuli-Responsive Microparticles. ACS Appl. Mater. Interfaces 2015; 7(18):9744-51.
20. Rahmani S, Lahann J. Recent progress with multicompartmental nanoparticles. MRS Bull. 2014; 39(3):251-7.
21. Yoon J, Kota A, Bhaskar S, Tuteja A, Lahann J. Amphiphilic Colloidal Surfactants Based on Electrohydrodynamic Cojetting. ACS Appl. Mater. Interfaces 2013; 5(21):11281-7.
22. Park BJ, Brugarolas T, Lee D. Janus particles at an oil-water interface. Soft Matter 2011; 7:6413-7.
23. Nie L, Liu S, Shen W, Chen D, Jiang M. One-pot synthesis of amphiphilic polymeric janus particles and their self-assembly into supermicelles with a narrow size distribution. Angew. Chem. Int. Ed. Engl. 2007; 46(33):6321-4.
24. Hong L, Cacciuto A, Luijten E, Granick S. Clusters of charged Janus spheres. Nano Lett. 2006; 6(11):2510-4.
25. Ma Y, Cao X, Feng X, Ma Y, Zou H. Fabrication of super-hydrophobic film from PMMA with intrinsic water contact angle below 90°. Polymer 2007;48(26):7455-7460.
26. Grundke, K. Surface-energetic properties of polymers in controlled architecture. In: Molecular Interfacial Phenomena of Polymers and Biopolymers. Ed. by P. Chen. Cambridge: Woodhead Publishing Limited 2005; 323-374.
27. Rotenberg Y, Boruvka L, Neumann AW. Determination of surface tension and contact angle from the shapes of axisymmetric fluid interfaces. J. Colloid Interface Sci. 1983; 93:169-83.

28. Fernandez-Rodriguez MA, Song Y, Rodriguez-Valverde MA, Chen S, Cabrerizo-Vilchez MA, Hidalgo-Alvarez R. Comparison of the Interfacial Activity between Homogeneous and Janus Gold Nanoparticles by Pendant Drop Tensiometry. Langmuir 2014; 30:1799-804.
29. Chi, L. (2010). Nanotechnology: Volume 8. Weinheim: Wiley-VCH.
30. Fernandez-Rodriguez MA, Chen L, Deming CP, Rodriguez-Valverde MA, Chen S, Cabrerizo-Vilchez M, Hidalgo-Alvarez R. A simple strategy to improve the interfacial activity of true Janus gold nanoparticles: a shorter hydrophilic capping ligand. Soft Matter 2016; 12:31-34.
31. Garbin V, Crocker JC, Stebe KJ. Particles at interfaces. J. Colloid Interface Sci. 2012; 387:1-11.

GRAPHICAL ABSTRACT